Check for updates

ARTICLE　　OPEN

Hippocampal Cofilin and CFL1 gene variants are linked to Alcohol Use Disorder phenotypes

Ahmad Salamian [1,10], Roberto Pagano [1,8,10], Edyta Skonieczna [1,10], Liubov S. Kalinichenko[2], Monika Puchalska [1], G. Yiğit Ünlü[1], Olga Gajewska-Woźniak [1], Lali Kruashvili[1], Małgorzata Grochowicz [1], Bartosz Wojtas [1], Bartek Gielniewski[1], Zofia Harda[1,9], Anna Cały [1], Christiane Mühle[2], Bernd Lenz [3], Johannes Kornhuber [2], Anbarasu Lourdusamy [4], Robbert Havekes[5], Ted Abel[6,7], Christian P. Müller [2] and Kasia Radwanska [1 ✉]

Alcohol use disorder (AUD) is characterized by pathological motivation to consume alcohol and cognitive inflexibility, leading to excessive alcohol seeking and use. In this study, we investigated the molecular correlates of impaired extinction of alcohol seeking during forced abstinence using a mouse model of AUD in the automated IntelliCage social system. This model distinguished AUD-prone and AUD-resistant animals based on the presence of ≥2 or <2 criteria of AUD, respectively. We used RNA sequencing to identify genes differentially expressed in the hippocampus, a brain region implicated in alcohol motivation, seeking during abstinence, and cognitive inflexibility. Our findings revealed differences in the hippocampal genes linked to the actin cytoskeleton and synaptic function, including cofilin (Cfl), and impaired synaptic transmission in the molecular layer of the hippocampal dentate gyrus (ML-DG) in ≥2 criteria mice as compared to <2 crit animals. To complement this data, we conducted local genetic manipulations in DG. Overexpression of Cfl in the polymorphic layer of the hippocampal dentate gyrus (PoDG) inhibited ML-DG synapses, increased motivation to seek alcohol and sucrose rewards, impaired extinction of seeking, and decreased reward consumption during relapse. Reducing Cfl levels had opposite effects. We also identified three SNPs in the human CFL1 gene (rs369270402, rs2376005, rs36124259) associated with increased AUD risk and found CFL1 mRNA blood levels correlated with alcohol-related hospital admissions. Overall, our study uncovers a novel mechanism linking hippocampal Cfl expression with AUD phenotypes and identifies CFL1 polymorphisms as AUD risk factor in humans.

Molecular Psychiatry; https://doi.org/10.1038/s41380-025-03226-3

INTRODUCTION

Alcohol use disorder (AUD) is a progressive and debilitating psychiatric disease characterized by pathological alcohol craving and motivation to consume alcohol, as well as cognitive rigidity. This condition results in an excessive focus on alcohol procurement and alcohol use in daily routines [1]. Although AUD is one of the leading causes of premature deaths globally, pharmacological interventions aiming to control alcohol misuse are limited, with significant negative side effects, and therefore infrequently prescribed and used [2–4]. To identify a new therapeutic approach to battle AUD, a neurobiology of the disease must be elucidated. So far most of the molecular studies focused on the quantitative aspects of alcohol use [5]- several candidate genes and molecular pathways that affect the amounts of consumed alcohol both in humans and animals have been identified [6–9]. Moreover, in recent years an accumulating number of studies focus on the

biology of complex alcohol-related behaviors, such as compulsivity [10–14], cognitive inflexibility [15], or choice between alcohol and natural rewards [16–18]. Still, the molecular processes that affect behavioral hallmarks of AUD beyond alcohol consumption remain poorly understood. To develop a successful prevention and therapeutic control of AUD progression, the neuronal basis of all AUD-related behaviors must be recognized.

Here we focused on the molecular correlates of excessive alcohol seeking induced in the alcohol-predicting context during alcohol withdrawal. Alcohol seeking during abstinence reflects individual focus on alcohol procurement and use, as well as cognitive inflexibility characteristic for AUD patients [1, 19]. Importantly, the predictive power of drug cues and contexts can be reduced by repeatedly presenting them in the absence of the alcohol reinforcer, a process known as extinction. The potential of extinction to limit relapse has generated considerable interest and research over the

past few decades [20–24]. The key brain circuits, including the prefrontal and insular cortices, amygdala, hypothalamus, striatum and hippocampus [22, 25–30], involved in the process of drug seeking extinction have been defined, however, the molecular processes that guide extinction are mostly unknown.

To look for the molecular mechanisms of alcohol seeking and its extinction, we used a mouse model of AUD that has been pharmacologically-validated [31–33] and proven to have significant translational value [34–36]. The model is based on four DSM-5 criteria of the disease [1, 31]. (i) Craving, or a strong desire or urge to use alcohol. We measured motivation to obtain alcohol in a progressive-ratio schedule. (ii) The subjects spend a great deal of time in activities necessary to obtain alcohol. We measured the extinction of alcohol seeking during periods of forced abstinence. (iii) The subject takes alcohol in larger amounts than intended. We measured alcohol intake during alcohol relapse after abstinence. (iv) Unsuccessful efforts to control alcohol use. We measured alcohol seeking induced by alcohol-predicting cues and during signaled periods of alcohol non-availability. The model allowed us to distinguish the animals that exhibit consistent AUD-prone phenotype, as they were positive (uppermost 30% of the population) in at least two AUD-related tests (≥ 2 crit mice), and the AUD-resistant mice that were positive in none or one test (< 2 crit animals). Next, we used the new generation RNA sequencing (RNA-seq) to characterize differentially expressed genes in the hippocampus of ≥ 2 crit and < 2 crit animals seeking for alcohol during alcohol withdrawal. We focused on the hippocampus as aberrant hippocampal synaptic plasticity is causally linked with cognitive and motivational aberrations characteristic for AUD, including drug seeking induced by drug-predicting contexts and cues [27, 29, 32, 33, 37–39]. In particular, the manipulations that ablate adult neurogenesis in DG increase drug consumption and motivation to seek for drugs, as well as invigorate drug seeking induced by associated cues and contexts [38, 39]. Moreover, the CA1 area and subiculum have been implicated in drug-induced place preference and context-induced alcohol and drug seeking during abstinence [27–29, 37, 40–42]. The molecular processes that underlie the functions of the hippocampus in extinction of alcohol seeking during abstinence are still largely unknown.

Our data showed that the variance in the transcriptome between the < 2 crit and ≥ 2 crit drinkers after alcohol withdrawal primarily involves hippocampal genes related to the cytoskeleton and synaptic function, including actin binding molecule, cofilin (Cfl) [43]. Accordingly, ex vivo electrophysiology was used to characterize pre- and post-synaptic changes in the hippocampus of the < 2 crit and ≥ 2 crit mice. We investigated the role of the hippocampal Cfl in the AUD phenotype using the local over-expression of Cfl and short hairpin mRNA specific for *cfl* mRNA delivered by viral vectors. Finally, we tested the predictive value of SNPs within the human *CFL1* gene and blood *CFL1* mRNA levels for AUD diagnosis. Overall, our study identifies transcriptomic differences between the AUD-prone vs -resistant drinkers during alcohol withdrawal. We also describe a novel mechanism that links Cfl-regulated synaptic plasticity in the hippocampus with AUD phenotype characterized by high motivation to seek for alcohol and impaired extinction of alcohol seeking during withdrawal and alcohol consumption during relapse. Finally, we identify CFL1 gene polymorphisms as an AUD risk factor and blood CFL1 levels as a predictor of alcohol-related hospital admissions.

MATERIALS AND METHODS
Mice
Ten-week old female and male C57BL/6J mice were purchased from the Medical University of Bialystok, Poland. Animals were housed under a 12/12 hr light/dark cycle in standard mouse home cages with *ad libitum* access to water and food. Experiments were approved by the Animal Protection Act of Poland guidelines and the 1st Local Ethical Committee in Warsaw, Poland (no. 117/2016, 421/2017, 884/2019). All experiments were planned to reduce the number of animals used and to minimize their suffering.

Animal model of AUD in the IntelliCages
The training in the IntelliCage was based on published protocol [31] and composed of the following phases: initiation of alcohol consumption in increasing concentrations, free access to 10% alcohol, motivation test, persistence test, withdrawal, cue relapse and alcohol relapse.

The details of the materials and methods used in the study are in the Supplementary Materials.

RESULTS
Characteristics of AUD-prone and -resistant mice
To identify AUD-prone and -resistant mice we used a mouse model of the disease in the social context of IntelliCages [31]. C57BL/6J female mice (n = 58) went through a long-term training consisting of the introduction of alcohol (4–12%, days 1–12) and alcohol free access period (FA, days 13–47). During the 4–12% and FA mice had unlimited access to alcohol in the reward corner. Alcohol consumption was tightly correlated with blood ethanol concentration (Supplementary Figure 1). Alcohol availability was signaled by the cue light presented each time a mouse entered the corner and each nosepoke in the corner gave access to alcohol for 5 seconds (fixed ratio 1, FR1). We also assessed behaviors that resemble DSM-5 criteria for AUD [1, 31]: high motivation to drink alcohol was measured as a number of nose-pokes in the reward corner performed in a progressive-ratio schedule of reinforcement test when mice had to make an increasing number of nosepokes (FR2, 4, 8, 12, 16, 20, 24, 28…) in order to get access to alcohol for 5 seconds (Motivation); excessive alcohol seeking was measured as number of nosepokes in the alcohol corner when the corner was inactive and nosepokes had no programmed consequences (Extinction); reactivity to alcohol-predicting cues was assessed as nosepokes in the alcohol corner during presentation of the cue light when alcohol was not available (Cue relapse) [44]; lack of control over alcohol consumption was assessed as alcohol consumption (g/kg/day) when the alcohol corner was activated after withdrawal (Alcohol relapse); while lack of control over alcohol seeking was measured as the change of nosepokes number to the alcohol corner during the non-active vs. active phases of the test (Persistence) (Fig. 1A). AUD score was calculated as a sum of normalized scores from all AUD tests, and AUD index as a sum of positive results (top 30%) in all tests [31, 45]. Mice were distinguished based on the DSM-5 criteria [1, 31]: AUD-prone drinkers were positive in at least two AUD tests (AUD Index ≥ 2 crit), AUD-resistant drinkers were positive for none or one criterion (AUD Index < 2 crit). Overall, 38% of the mice were indicated as AUD-prone drinkers (Fig. 1B).

Retrospective analysis of the mice behavior showed that the ≥ 2 crit group, as compared to the < 2 crit animals, had higher AUD score as well as scores in all AUD tests (Supplementary Figure 2). Moreover, AUD index correlated with AUD score (Fig. 1C) and all AUD-related behaviors (Fig. 1D), but not alcohol consumption or mice activity (Fig. 1E, F). The paradoxical lack of correlation between the AUD index and alcohol consumption may stem from our analysis of daily alcohol consumption throughout the entire training period. Based on our observations, all mice initially consume similar amounts of alcohol, but the < 2 crit animals gradually reduce their alcohol intake over time. The < 2 crit and ≥ 2 criteria mice only begin to differ in alcohol consumption toward the end of the study. Therefore, we believe that our analysis of alcohol consumption in mice more accurately reflects the very early stages of alcohol use in young adults, rather than compulsive drinking observed in AUD patients.

Interestingly, we did not observe significant correlation between some AUD behaviors (Fig. 1G, e.g. M vs E, AR and P),
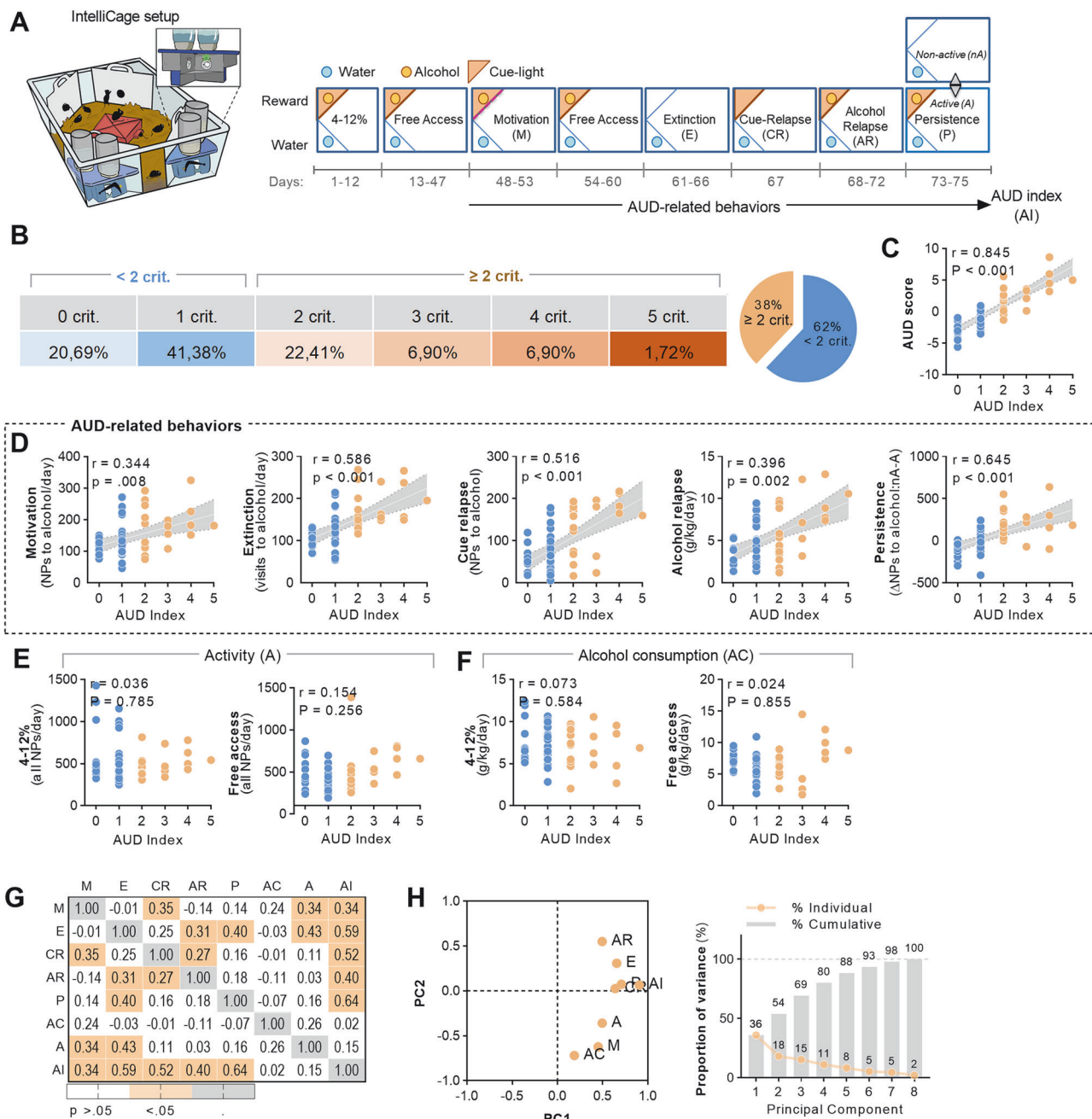
Fig. 1 AUD-related behaviors of the < 2 crit and ≥ 2 crit drinkers. (A) IntelliCage setup and experimental timeline. Mice (n = 58) were habituated to the cage, trained to drink alcohol (4–12%) and AUD-related behaviors were tested: motivation to drink alcohol (M), extinction of alcohol seeking during withdrawal (E), alcohol seeking during cue relapse (CR), alcohol drinking during alcohol relapse (AR), and alcohol seeking during a persistence test (P). During the periods of free access to alcohol (FA) mice had unlimited access to alcohol (10%). Alcohol availability was signaled by a cue light in a reward corner. **(B)** Frequency of < 2 crit and ≥ 2 crit drinkers and **(C)** Spearman correlations between AUD Index and AUD score. $n_{total} = 58$, $n_{AI0} = 12$, $n_{AI1} = 24$, $n_{AI2} = 13$, $n_{AI3} = 4$, $n_{AI4} = 4$, $n_{AI5} = 1$. **(D)** Spearman correlations between AUD Index (AI) and AUD-related behaviors. Each dot on the graphs represents one animal. Linear regression lines ± 95% confidence intervals are shown; Spearman correlation (r) and ANCOVA results are given for raw data. **(E, F)** Spearman correlations between AUD Index, **(E)** mice activity and **(F)** alcohol consumption during 4–12% and FA phases. Each dot on the graphs represents one animal. Linear regression lines ± 95% confidence intervals are shown; Spearman correlation (r) and ANCOVA results are given for raw data. **(G)** Spearman correlations (r) between AUD index (AI) and AUD-related behaviors, activity (A) and alcohol consumption (AC). **(H)** Principal component analysis (PCA) of AUD behaviors. Each dot on the PCA graph (left) represents one behavioral measure [motivation to drink alcohol (M), extinction of alcohol seeking during withdrawal (E) and cue relapse (CR), alcohol drinking during alcohol relapse (AR), alcohol seeking during a persistence test (P), activity (A) and alcohol consumption (AC)]. (right) Proportion of variance explained by PCs.

suggesting that these behavioral traits are independent and driven by different neuronal mechanisms. However, all AUD behaviors had positive association with the main factor (PC1) in the principal components analysis (PCA) (Fig. 1H and

Supplementary Table 1), indicating that PC1 represents AUD-like alcohol seeking.

Thus, the AUD model allowed for the identification of the mice that demonstrate a AUD-like phenotype and AUD-resistant
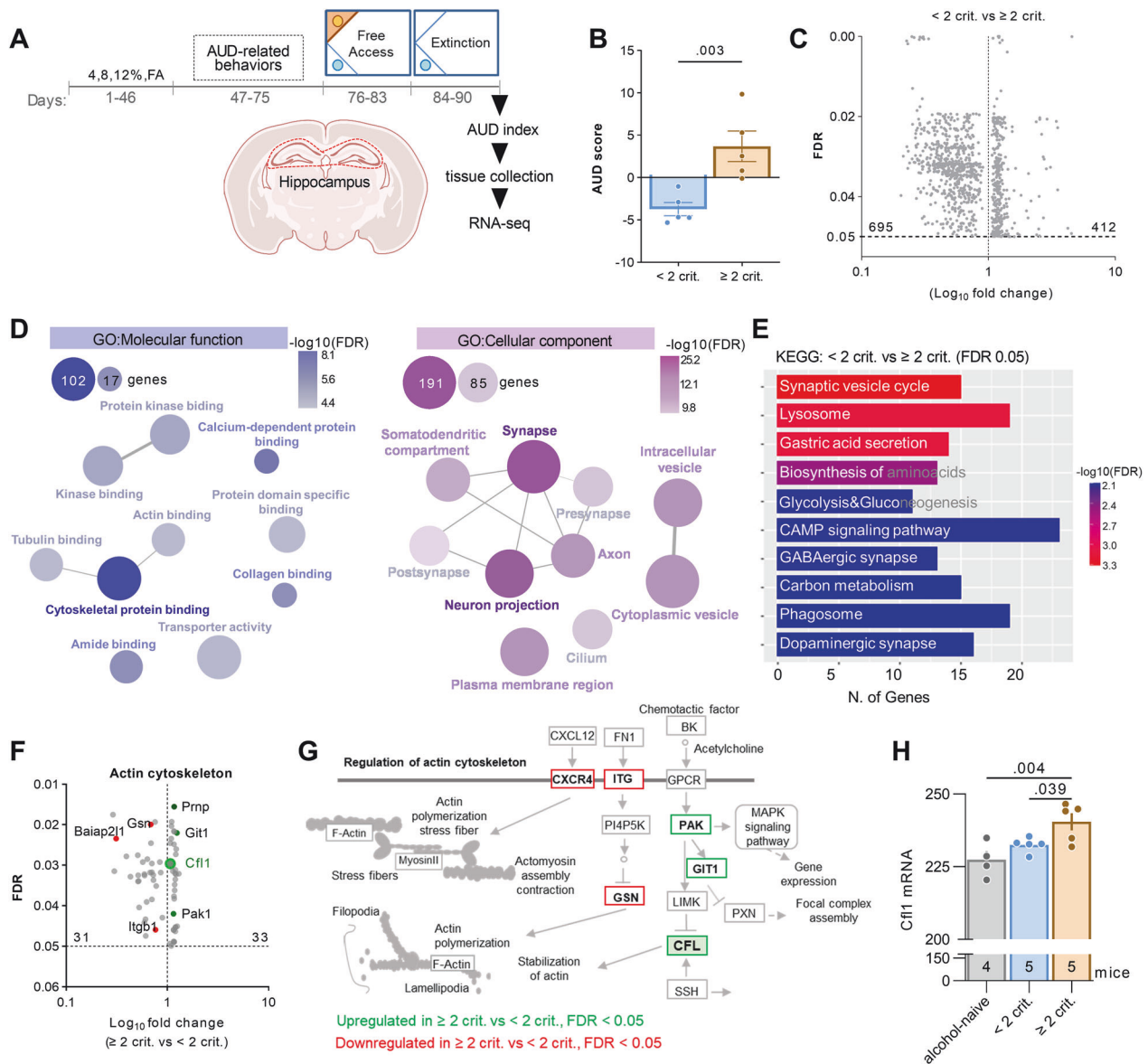
Fig. 2 Transcripts related to cytoskeleton and synaptic function are differentially expressed in the hippocampus of the < 2 crit and ≥ 2 crit drinkers during extinction of alcohol seeking. (A, B) Experimental timeline. Mice were trained to drink alcohol in the IntelliCages (n = 16), classified as < 2 crit (n = 5) and ≥ 2 crit drinkers (n = 5) and sacrificed after a second alcohol extinction test (day 90) (AUD score: t(8) = 3.78, p = 0.003). Hippocampus tissue was dissected from fresh brains for RNA-seq analysis. **(C)** A volcano plot illustrating DEGs in the hippocampus of < 2 crit and ≥ 2 crit drinkers. Only genes with FDR < 0.05 are shown. **(D)** Gene ontology analysis of molecular function (GO:MF) and cellular components (GO:CC) based on the genes deregulated (both up- and downregulated) in the hippocampus of < 2 crit vs. ≥ 2 crit drinkers (FDR cutoff 0.05). The network shows pathways in nodes. Two nodes are connected if they share 20% or more genes. Darker nodes are more significantly enriched gene sets while bigger nodes represent larger gene sets. Thicker connection between nodes represents more overlapped genes. **(E)** KEGG pathway analysis of the deregulated genes (both up- and downregulated) in the hippocampus of < 2 crit vs. ≥ 2 crit drinkers (FDR cutoff 0.05). **(F)** A volcano plot illustrating DEGs from Cytoskeletal protein binding,Tubulin binding and Actin binding nodes (GO:MF) in the hippocampus of < 2 crit vs. ≥ 2 crit drinkers. **(G)** Regulation of actin cytoskeleton pathway (KEGG) with indicated DEGs in the hippocampus of < 2 crit and ≥ 2 crit drinkers. **(H)** Cofilin (Cfl) mRNA levels in the hippocampus of alcohol-naive, < 2 crit and ≥ 2 crit drinkers (One-way ANOVA, F(2, 11) = 6.96, p = 0.011). Data are presented as means +/- SEM.

drinkers. As extinction of alcohol seeking during alcohol withdrawal was a good predictor of AUD phenotype and heavily loaded on PC1, in the following step we focused on transcriptomic differences between the < 2 crit and ≥ 2 crit mice following withdrawal.

Differentially expressed genes in the hippocampus of ≥ 2 crit and < 2 crit mice during extinction of alcohol seeking

We hypothesized that transcriptomic differences drive the variance between the < 2 and ≥ 2 crit mice in extinction of

alcohol seeking during alcohol withdrawal. To test this hypothesis 16 female mice were trained to drink alcohol in the IntelliCages. For the molecular analysis ten individuals with the highest (≥ 2 crit, n = 5) and lowest AUD index (< 2 crit mice, n = 5) were selected (Fig. 2A). They differed in AUD score as well as all AUD behaviors including extinction of alcohol seeking during withdrawal (Fig. 2B and Supplementary Figure 3). The hippocampus tissue was collected immediately after the second alcohol extinction test (day 90, Fig. 2A), total RNA was extracted and used for a new generation high-throughput RNA sequencing

(RNA-seq). We focused on this brain region as the hippocampus has been implicated in context-induced alcohol and drug seeking during withdrawal [27–29, 37, 40–42].

The hippocampal transcriptome analysis of ≥ 2 crit and < 2 crit mice yielded 1107 differentially expressed genes (DEGs); 412 genes were upregulated and 695 downregulated in ≥ 2 crit as compared to < 2 crit animals (Fig. 2C). Next, the hippocampal DEGs were classified according to their molecular function (MF) and cellular component (CC) categories by the gene-ontology (GO) platform [46]. GO enrichment analysis of DEGs mapped a large proportion of the genes into the *cytoskeletal function* (GO:MF, 102/987 genes, FDR = 5.10E^{-12}) and *synapse* localisation (GO:CC, 191/1465 genes, FDR = 3.20E^{-39}) (Fig. 2D, Supplementary Table 2, 3). According to the Kyoto Encyclopedia of Genes and Genomes (KEGG) [47] the *synaptic vesicle cycle* pathway was the most differentially expressed (Fig. 2E, Supplementary Table 4) (15/77 genes, FDR = 0.00048). These results indicate that the reorganization of the cytoskeleton and changes in synaptic function in the hippocampus may contribute to differences in extinction of alcohol seeking between the < 2 and ≥ 2 crit mice.

Cfl is upregulated in the hippocampus of the ≥ 2 crit mice during extinction of alcohol seeking

Among the top DEGs associated with the cytoskeleton function, we found upregulation of cofilin (Cfl) transcripts in the ≥ 2 crit mice as compared to < 2 crit animals (Fig. 2F–H) and the Cfl mRNA levels correlated with alcohol seeking during cue relapse, extinction test and with AUD index (Supplementary Figure 3D). Previous studies have shown that Cfl severs actin filaments, leading to increased actin cytoskeletal dynamics [48]. This mechanism not only regulates postsynaptic function but also synaptic vesicle mobilization and exocytosis [49–51]. Additionally, active Cfl can bind to F-actin and form stable actin rods, which can impede axonal trafficking [52]. Since RNA-seq analysis suggests that these processes may be dysregulated in the hippocampus of ≥ 2 crit mice during alcohol withdrawal (Fig. 2D, E) we chose to focus on Cfl in the subsequent steps of our study.

To verify distinctive expression of Cfl in the ≥ 2 crit and < 2 crit groups during extinction test, female mice were trained to drink alcohol in the IntelliCages. The ≥ 2 crit and < 2 crit animals were identified and they were sacrificed after 7-day alcohol withdrawal (extinction, day 90) (Supplementary Figure 4). The brains were sliced and immunostained with specific antibodies. We analyzed Cfl levels on the brain slices as integrated mean gray values of the microphotographs. Significant upregulation of Cfl in the ≥ 2 crit, as compared to < 2 crit mice, was observed in the dentate gyrus of the hippocampus (DG), but not CA1 area, basolateral amygdala (BLA), central nucleus of the amygdala (CeA), nucleus accumbens (NAc) and caudate putamen (CaPu) (Supplementary Figure 4D, E).

To confirm this observation the experiment was repeated with a new cohort of female mice. The ≥ 2 crit and < 2 crit mice were sacrificed during free alcohol access period (alcohol, day 83) or after 7-day extinction test (extinction, day 90) (Supplementary Figure 5, Fig. 3A and B). We also used alcohol-naive mice as a control. We focused on the analysis of Cfl in the DG layers: the granule cell layer (GCL), polymorphic layer of dDG (PoDG), as well as the molecular layer of GC dendrites (ML) (Fig. 3C). Overall, Cfl levels were increased in all mice drinking alcohol as compared to alcohol-naive animals. Furthermore, the levels of Cfl were increased in the ML and PoDG after extinction test in the ≥ 2 crit mice, as compared to the < 2 crit extinction animals and the ≥ 2 crit alcohol group (Fig. 3D), and Cfl levels in all DG strata correlated with alcohol seeking during extinction and AUD index (Supplementary Figure 5D). Similar correlation between Cfl levels, Extinction and AUD index was also observed in male mice sacrificed after Extinction (Supplementary Figure 5E).

As RNA-seq analysis suggested deregulation of the synaptic proteins and proteins related to synaptic vesicle cycle in the ≥ 2

mice (Fig. 2E), we also analyzed colocalization of Cfl with synaptotagmin 1 (Syt1) (Ca^{2+} sensor in the membrane of the pre-synaptic axon terminal involved in both synaptic vesicle docking and fusion with the presynaptic membrane; upregulated in RNA-seq data, Supplementary Table 2) and PSD-95/Dlg4 (post-synaptic scaffold protein; upregulated in RNA-seq data, Supplementary Table 2) (Fig. 3E, F). Overall, synaptic Cfl levels (Cfl colocalizing with Syt1 and PSD-95) were increased in mice drinking alcohol as compared to alcohol-naive mice. We also observed increased levels of Cfl colocalized with Syt1 in the ML in the ≥ 2 crit mice after extinction, as compared to the ≥ 2 crit alcohol group and the < 2 crit extinction animals (Fig. 3E). There was no significant effect of the training and AUD on the levels of Cfl co-localised with PSD-95 (Fig. 3F). Altogether, our analysis shows that alcohol training upregulates Cfl in DG. Furthermore, extinction of alcohol seeking upregulates Cfl in PoDG and ML in the ≥ 2 crit mice as compared to the < 2 group; and the upregulated Cfl in ML colocalized with the pre- but not post-synaptic compartments.

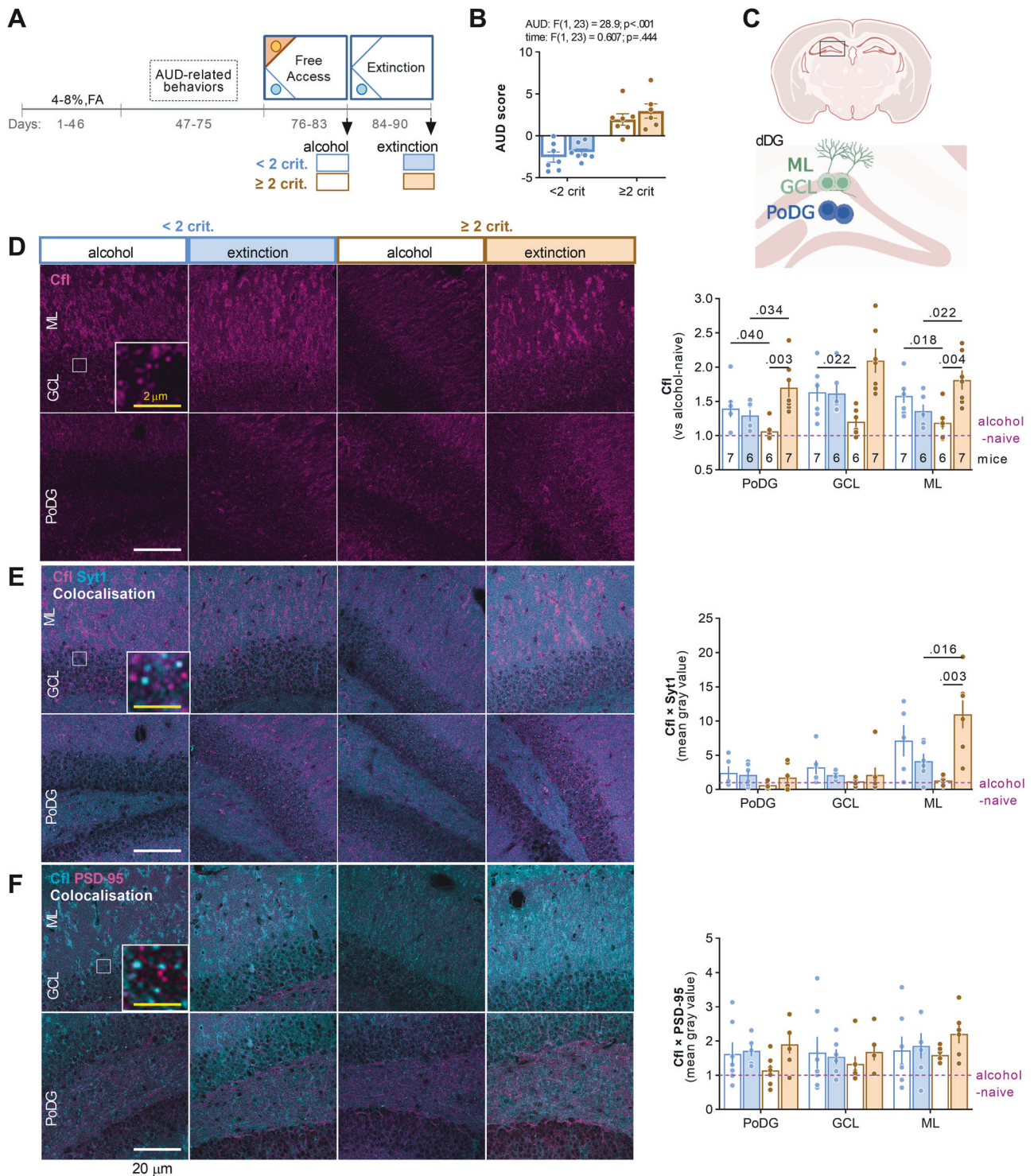### Extinction of alcohol seeking impairs ML synaptic function in ≥ 2 crit mice

To test whether extinction of alcohol seeking induces synaptic changes in the ML of the ≥ 2 crit mice, we trained a new cohort of female mice to drink alcohol in the IntelliCages. As previously, ≥ 2 and < 2 crit mice were identified and sacrificed during FA (alcohol) or after extinction test (Fig. 4A and B, Supplementary Figure 6). Alcohol-naive mice were used as a control. Field excitatory postsynaptic potentials (fEPSPs) were recorded to evaluate synaptic function by measuring input-output and paired-pulse ratio (PPR) in the ML synapses of acute hippocampal slices when axons terminating in the ML were stimulated by monotonically increasing stimuli (Fig. 4C).

The PPR slope was significantly decreased in the alcohol mice as compared to alcohol-naive animals, and increased in the ≥ 2 crit mice sacrificed after extinction test, as compared to the < 2 crit extinction animals and the ≥ 2 crit alcohol mice (Fig. 4D, E). This data indicates higher presynaptic release probability in the alcohol mice, as compared to the alcohol-naives, and lower in the ≥ 2 crit mice after extinction as compared to other alcohol groups. PPR slope correlated with alcohol seeking during persistence and extinction tests and AUD index (Supplementary Figure 6D). Moreover, the input-output curves for the slope of fEPSP were increased in the alcohol mice as compared to alcohol-naives, and decreased in the ≥ 2 crit extinction mice compared to the ≥ 2 crit alcohol group and < 2 crit extinction mice (Fig. 4F-H), suggesting more synaptic transmission in the alcohol groups as compared to alcohol-naive animals, and less synaptic transmission in the ≥ 2 crit extinction mice as compared to other alcohol groups. fEPSP slope negatively correlated with alcohol seeking during cue relapse and positively with alcohol consumption during relapse (Supplementary Figure 6D). We also observed lower fiber volley (FV) responses in the ≥ 2 crit mice as compared to the alcohol-naive and < 2 crit animals indicating less activated axons in the ≥ 2 crit mice.

Overall, higher PPR and lower input-output in the alcohol-naive mice as compared to alcohol-trained animals indicate increased synaptic function after alcohol training. However, higher PPR and lower input-output in the ≥ 2 crit mice after extinction test, as compared to the < 2 crit extinction group and the ≥ 2 crit alcohol animals, indicate weakening of the ML synapses of ≥ 2 crit mice during alcohol withdrawal. This process is likely driven by pre-synaptic changes.

Overexpression of cofilin in PoDG weakens contralateral synapses in the ML of DG

The main inputs to the ML originate from the entorhinal cortex and contralateral PoDG (Fig. 4C). As we observed increased Cfl

Figure with panels A–F.

levels in PoDG of the ≥ 2 crit mice after extinction (Fig. 3D) we hypothesized that weakened synaptic transmission in the ML of the ≥ 2 crit mice after extinction test, as compared to the ≥ 2 crit mice before extinction, is driven by the increase of presynaptic Cfl levels in PoDG. To address this hypothesis, alcohol-naive female mice were unilaterally injected into DG with adeno-associated viral vectors (AAV$_{2.1}$) expressing cofilin with hemagglutinin tag (HA) (Cfl) under CaMKII promoter [53]. This resulted in Cfl overexpression in the PoDG cells (Cfl_PoDG) ipsilateral to the injection, and in the PoDG axons in the ML (Cfl_ML) contralateral

to the injection (Fig. 5A–D). The AAV$_{2.1}$ encoding eGFP under CaMKII promoter was used as a control. The fEPSPs were recorded to measure input-output and PPR in the ML while axons terminating in the ML were stimulated (Fig. 5D).

The PPR, analyzed as slope of fEPSP, was significantly increased in the Cfl_ML slices, as compared to the eGFP and the Cfl_PoDG sections (Fig. 5E). The fEPSP slope of the input-output test was significantly decreased in the Cfl_ML slices compared to the eGFP and Cfl_PoDG slices. We did not observe the difference in the ML synaptic strength in the Cfl_PoDG slices compared to the eGFP

Fig. 3 Cfl is upregulated in DG of the ≥ 2 crit animals during extinction of alcohol seeking. (**A**, **B**) Experimental timeline. Mice were trained to drink alcohol (n = 26) or water (alcohol-naive, n = 8) and AUD-related behaviors were tested. (**B**) AUD scores were calculated to identify the < 2 crit vs ≥ 2 crit drinkers. < 2 crit vs. ≥ 2 crit mice significantly differed in alcohol seeking during withdrawal (Mann Whitney test, U = 2). Mice were sacrificed and perfused after free alcohol access period (day 83) or alcohol withdrawal (day 90). The brains were cut and brain sections immunostained to detect cofilin (Cfl). (**C**) Schematic representation of the analyzed dDG regions. GCL, granule cell layer; PoDG, polymorphic layer of DG; ML, molecular layer. (**D**) The analysis of Cfl fluorescent immunostaining. Representative microphotographs and summary of data (repeated measures three-way ANOVA with Šídák's multiple comparisons test, effect of region: $F_{(1,40, 30,8)} = 16.6$, $p < 0.001$; effect of phenotype: $F_{(1, 23)} = 0.169$, $p = 0.685$; effect of time: $F_{(1, 23)} = 7.33$, $p = 0.013$; effect of region × AUD: $F_{(2, 44)} = 0.0189$, $p = 0.981$; effect of region × time: $F_{(2, 44)} = 3.36$, $p = 0.044$; effect of phenotype × time: $F_{(1, 23)} = 14.2$, $p = 0.001$. (**E**) The analysis of Cfl colocalization with presynaptic marker, synaptotagmin 1 (Syt1). Representative microphotographs and summary of data (repeated measures three-way ANOVA with Šídák's multiple comparisons test, effect of region: $F_{(1.71, 34.3)} = 26.3$, $p < 0.001$; effect of phenotype: $F_{(1, 22)} = 0.598$, $p = 0.447$; effect of time: $F_{(1, 22)} = 1.88$, $p = 0.184$; effect of region × phenotype: $F_{(2, 40)} = 0.919$, $p = 0.184$; effect of region × time: $F_{(2, 40)} = 4.04$, $p = 0.025$; effect of phenotype × time: $F_{(1, 22)} = 11.8$, $p = 0.002$. (**F**) The analysis of Cfl colocalization with a postsynaptic marker, PSD-95. Representative microphotographs and summary of data (repeated measures three-way ANOVA, effect of region: $F_{(1.84, 40.5)} = 4.59$, $p = 0.018$; effect of phenotype: $F_{(1, 22)} = 0.0296$, $p = 0.865$; effect of time: $F_{(1, 22)} = 1.34$, $p = 0.259$; effect of region × phenotype $F_{(2, 44)} = 0.836$, $p = 0.440$; effect of region × time: $F_{(2, 44)} = 1.27$, $p = 0.292$; effect of phenotype × time: $F_{(1, 22)} = 1.06$, $p = 0.315$. Mean ± SEM are shown. For B, D-F each dot on the graphs represents one animal.

sections (Fig. 5F). We also did not observe any effect of the virus on FV amplitude (Fig. 5F). Thus, overexpression of Cfl in the PoDG cells decreased the probability of synaptic release and synaptic transmission in the contralateral PoDG→ML synapses. This indicates that increased expression of Cfl in the PoDG→ML synapses is a plausible mechanism that decreases ML synaptic function in the ≥ 2 crit mice during alcohol withdrawal.

Effects of cofilin in PoDG on AUD-related behaviors and sucrose seeking

To test whether PoDG Cfl affects AUD-related behaviors, female mice were bilaterally injected with Cfl or the control eGFP virus. Two weeks after the surgery the animals started long-term alcohol training in the IntelliCages (Cfl, n = 13; eGFP, n = 12). To control whether the effects of Cfl in PoDG are specific for alcohol reward a separate cohort of mice was trained to drink sucrose (Cfl, n = 15; eGFP, n = 14) (Fig. 6A). Post-training analysis of the hippocampal sections showed that PoDG cells expressing Cfl had higher levels of Cfl and F-actin as compared to the non-transduced cells analyzed in the same animals [Cfl(-)]. Thus Cfl affected the actin cytoskeleton (Fig. 6B, C).

Overexpression of Cfl in PoDG increased motivation for alcohol and sucrose, and impaired extinction of alcohol and sucrose seeking during withdrawal (Fig. 6D and G). Cfl also decreased alcohol and sucrose consumption during relapse. It had, however, no effect on alcohol and sucrose seeking during cue relapse, persistence test and consumption of alcohol and sucrose during free access periods (Fig. 6D and G). Furthermore, PoDG Cfl had no effect on mice general activity in the water corner, total visits, nosepokes and liquid consumption (Supplementary Figure 7). Thus our data indicates that Cfl expression in PoDG regulates extinction of both alcohol and sucrose reward seeking, as well as reward motivation. As DG is also involved in extinction of aversive memories [54] these observations may suggest that Cfl in PoDG in general regulates learning, memory and extinction of all salient behaviors. To validate this hypothesis we tested if Cfl overexpression in PoDG affects extinction of contextual fear. We found, however, no effect of Cfl overexpression neither on contextual fear memory formation nor extinction (Supplementary Figure 9). Hence, our data suggests that the effect of Cfl in PoDG is specific for extinction of behaviors motivated by rewarding stimuli.

Finally, we tested whether slow extinction of alcohol seeking during abstinence can be improved by depleting Cfl levels in DG. To this end we used lentiviral vectors (LV) encoding short hairpin mRNA specific for cfl (shCfl, n = 15) or luciferase as a control (shLuc, n = 14). shCfl significantly decreased Cfl levels in the transduced cells (Fig. 7A) and, when injected into PoDG, decreased PPR in ML (Supplementary Figure 10). The viral vectors were injected in PoDG and 14 days after the surgery mice were

trained in the IntelliCages (Fig. 7B). During data analysis the shCfl and shLuc groups were divided into poor and good performers in each AUD test independently (bottom 70% and top 30% of the populations, respectively). This decision was motivated by two observations. Firstly, Cfl levels were upregulated during extinction only in mice with the highest extinction scores (Fig. 3D). Secondly, our behavioral analysis revealed that AUD-related behaviors were largely independent and poorly predictive of one another (Fig. 1G), suggesting that these behaviors are likely driven by distinct neuronal mechanisms. shCfl significantly decreased alcohol seeking of the top 30% groups during the extinction and cue relapse, and increased alcohol consumption during alcohol relapse (Fig. 7D). It had, however, no effect on alcohol consumption during free access periods (Fig. 7C and Supplementary Figure 9C), motivation and persistence of the top 30% group, performance of the bottom 70% group in all AUD tests (Fig. 7D), as well as mice activity and performance in the water corner except for the cue relapse when shCfl mice were in general less active (Supplementary Figure 9). Hence, our data indicate that Cfl in PoDG bidirectionally regulates alcohol seeking during abstinence and alcohol consumption during relapse.

Genome-wide association study (GWAS) of *CFL1* gene in AUD

In order to translate animal findings into the human condition we searched for a potential link between single nucleotide polymorphisms (SNPs) in the CFL1 gene with AUD. We used the coordinates of CFL1 gene from the Ensembl GRCh37 (release 75) database and extended it by 10KB. We extracted all SNPs and their corresponding summary statistics for this region. There were 44 SNPs, of which three [rs369270402 (AGAAG:AGAAGGAAG, Z = 2.951, P = 0.003), rs2376005 (A:G, Z = 2.945, P = 0.003) and rs36124259 (C:G, Z = 2.864, P = 0.004)], located in the intron and resulting in non-coding transcript variant, showed modest association with enhanced rates of alcohol dependence at the FDR less than 6.2%. These data suggest that mutations in CFL1 gene contribute to the risk of AUD development in humans.

CFL mRNA expression in AUD

In order to test whether CFL1 blood mRNA levels predict AUD in humans, we tested CFL1 mRNA expression in a cohort of 183 withdrawal seeking early-abstinent AUD patients from the bi-centric, cross-sectional, and prospective Neurobiology of Alcoholism (NOAH) study and compared to 197 age-matched healthy controls (Supplementary table 5). Results show no significant difference in CFL1 mRNA expression in AUD patients, neither at the hospital admission nor after 5-day detoxification (Supplementary Figure 11). There were also no sex differences between male and female AUD patients in blood CFL1 mRNA levels (Supplementary Figure 11). We found no significant correlations between
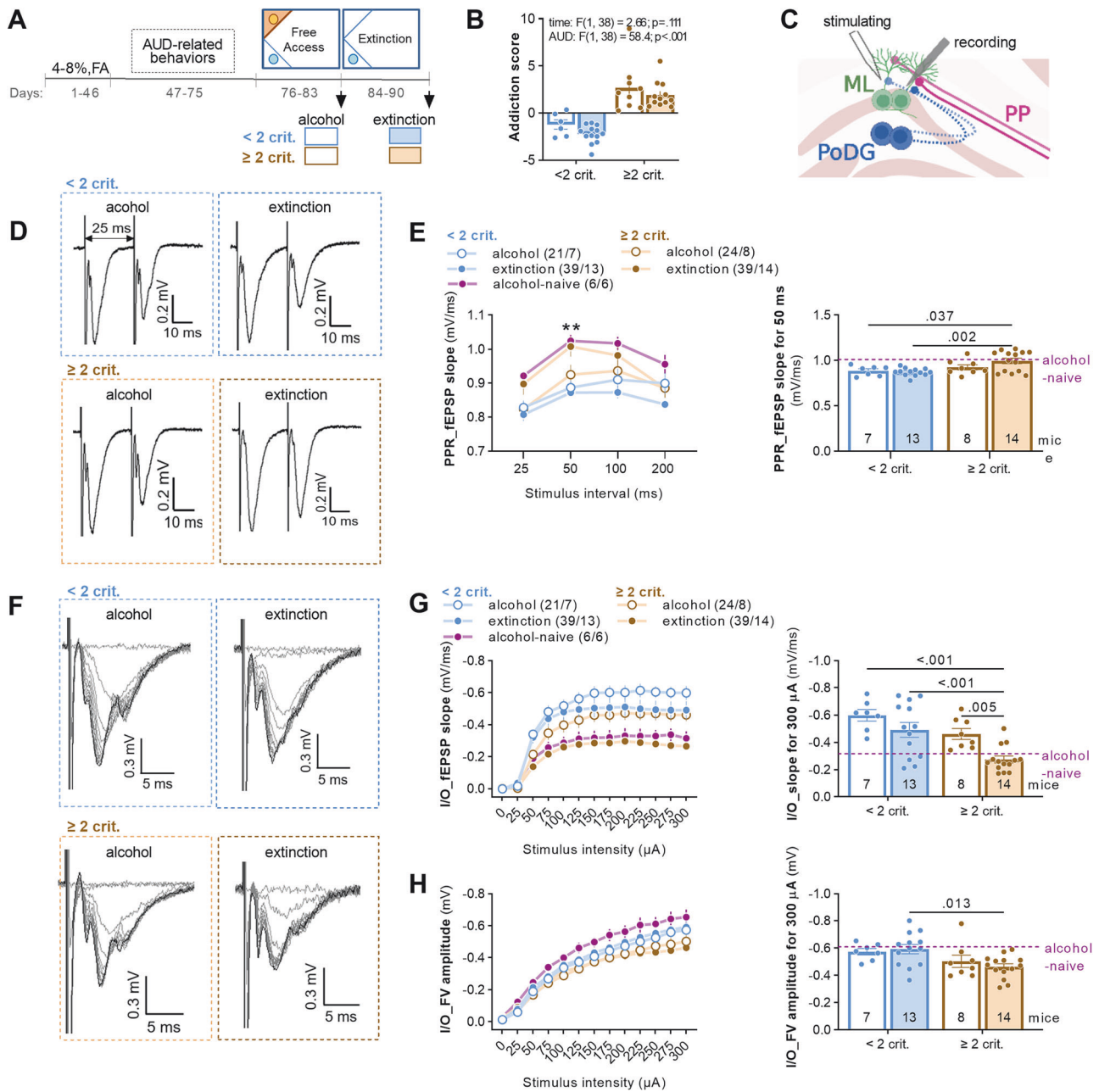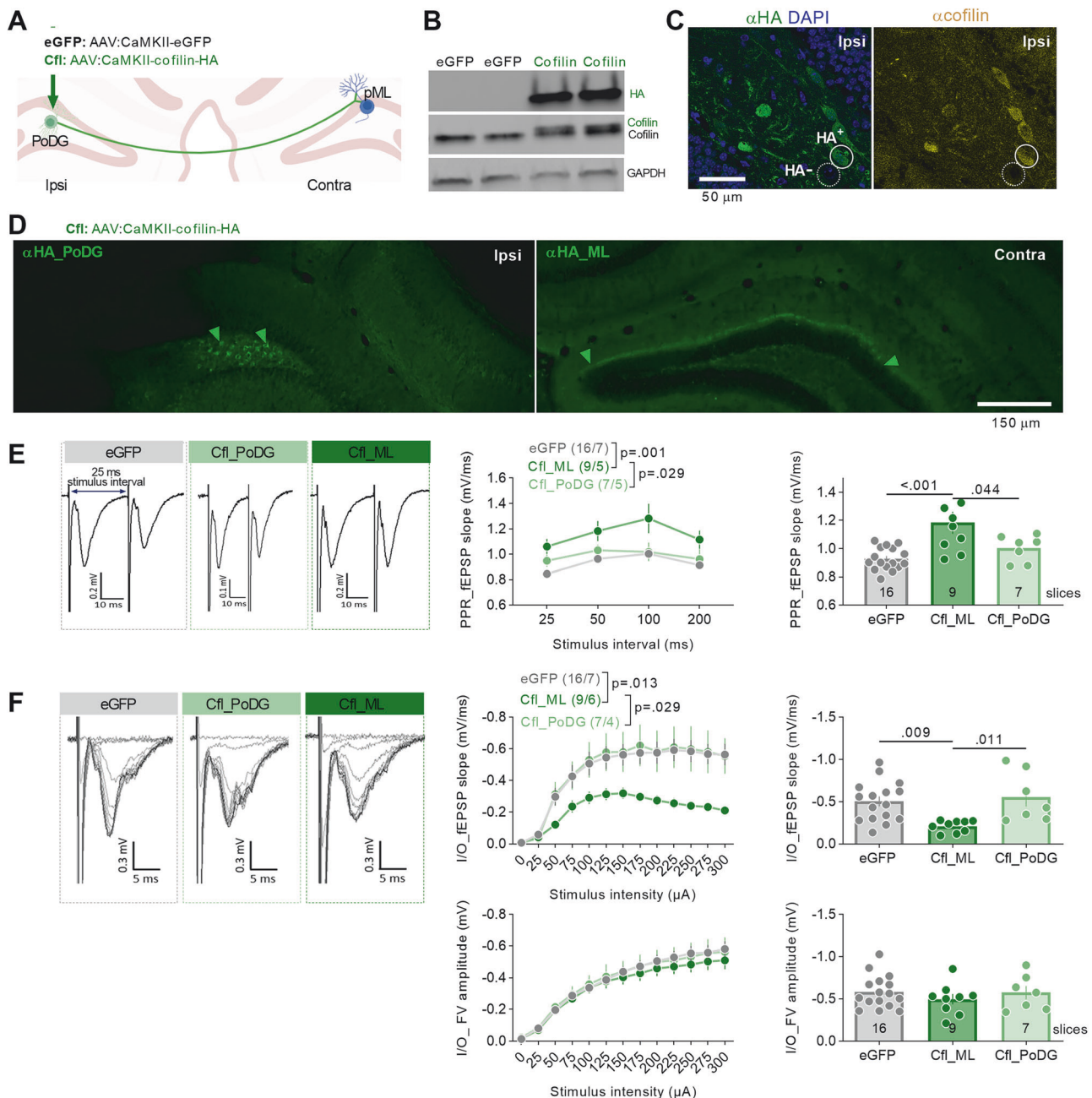
Fig. 4 Extinction of alcohol seeking impairs synaptic transmission in the ML of the ≥ 2 crit mice. (**A**, **B**) Experimental timeline. Mice were trained to drink alcohol (n = 42) or water (n = 6) and (**B**) AUD scores were calculated to identify the < 2 crit vs ≥ 2 crit drinkers. < 2 crit vs. ≥ 2 crit mice significantly differed in alcohol seeking during withdrawal (Mann Whitney test, U = 2). Mice were sacrificed after the period of free access to alcohol (day 83) or alcohol withdrawal (day 90). Alcohol-naive mice trained in the IntelliCage were used as a control. (**C**) Schematic representation of dDG. Field excitatory postsynaptic potentials (fEPSPs) were recorded in the molecular layer of dDG (ML_dDG) in response to the stimulation of the axons terminating in the ML: perforant pathway (PP) axons from the entorhinal cortex and axons from the contralateral polymorphic layer of DG (PoDG). (**D-H**) The analysis of synaptic responses. (**D**) Example of PPR traces of fEPSPs with 25 ms interstimulus interval. (**E, right**) Summary of data for PPR fEPSP slope recorded for different inter-stimulus intervals (25, 50, 100, 200 ms) (top, repeated measure two-way ANOVA, effect of stimulation intensity, $F(2.29, 86.9) = 21.7$, $p < 0.001$; treatment effect, $F(3, 38) = 2.94$, $p = 0.046$; treatment × stimulation interaction, $F(9, 114) = 2.50$, $p = 0.012$). (**E, left**) Summary of data for PPR fEPSP slope recorded for 50 ms interval (top, two-way ANOVA with Šídák's multiple comparisons test, phenotype effect, $F(1, 38) = 9.56$, $p = 0.004$, time effect, $F(1, 38) = 1.13$, $p = 0.295$). (**F**) Representative fEPSPs traces evoked by stimuli of different intensities. (**G, left**) Summary of data for input–output plots of fEPSP slope recorded in response to increasing intensities of stimulation (repeated measure three-way ANOVA, effect of phenotype: $F(1, 37) = 18.2$; $p < 0.001$; effect of time, $F(1, 37) = 8.47$; $p = 0.006$). (**G, right**) Summary of data for fEPSP slope elicited by 300 µA stimulus intensity (two-way ANOVA with Šídák's multiple comparisons test, effect of phenotype: $F(1, 38) = 15.1$, $p < 0.001$; effect of time: $F(1, 38) = 10.5$, $p = 0.003$). (**H, left**) Summary of data for fiber volley (FV) amplitude recorded in response to increasing intensities of stimulation (repeated measure three-way ANOVA, phenotype: $F(1, 38) = 6.22$, $p = 0.017$; time: $F(1, 38) = 0.162$, $p = 0.689$). (**right**) Summary of data for FV slope elicited by 300 µA stimulus intensity (two-way ANOVA with Šídák's multiple comparisons test, effect of phenotype: $F(1, 38) = 8.84$, $p = 0.005$; effect of time, $F(1, 38) = 0.102$; $p = 0.751$). Numbers of slices/animals per group are indicated in the legends. Data are presented as means of a group +/- SEM.

CFL1 blood mRNA levels and biochemical parameters of blood (including the ones showing liver condition that are important after chronic alcohol consumption such as AST, ALT, LDH, alcohol phosphatase, homocysteine, GammaGT) ($p < 0.05$), lifetime or daily alcohol drinking, scores of Obsessive Compulsive Drinking Scale (OCDS) or Penn Alcohol Craving Scale (PACS) (Table 1). We observed, however, that CFL1 mRNA levels in the blood collected after 5-day detoxification predicted the number of alcohol-related readmissions during 2-year follow-up and days to the first alcohol-related re-admission (Table 1). These findings indicate that peripheral cofilin level is not a marker of AUD, however it predicts alcohol-related readmissions to hospital. Thus overall our study indicates that peripheral CFL levels in human patients and hippocampal Cfl in mice predict how individuals will handle alcohol seeking during abstinence and alcohol use during relapse.

DISCUSSION

Previous studies linked multiple brain regions, including the prefrontal and insular cortices, amygdala, hypothalamus, striatum and hippocampus [22, 25–30], and receptor systems, including dopamine, opioid, noradrenaline, GABA, glutamate, with extinction of alcohol and drug seeking [55–58]. Still the molecular mechanisms that contribute to extinction of alcohol and drug seeking are mostly unknown. In this study, we characterized transcriptomic differences in the hippocampus during extinction of alcohol seeking between mice meeting the criteria for AUD (≥2 crit drinkers) and mice consuming alcohol without AUD diagnosis (<2 crit drinkers). Differential expression of genes associated with actin cytoskeleton reorganization and the synaptic vesicle cycle (e.g., Cfl1) in the hippocampus significantly contributed to the distinction between these phenotypes. Additionally, we observed

A. Salamian et al.

Fig. 5 Overexpression of cofilin in PoDG weakens strength of the contralateral PoDG → ML synapses. (A) Mice received dDG-targeted unilateral stereotactic injections of AAV encoding cofilin-HA under CaMKII promoter (Cfl, n = 7), or eGFP as a control (n = 7). **(B)** Blot shows the expression of endogenous cofilin in dDG (recognized by α-cofilin antibody), and exogenous cofilin-HA protein (green, detected by α-HA antibody and as a band shifted upwards on the α-cofilin blot). GAPDH was used as a loading control for WB. **(C)** Representative microphotographs of the α-HA and α-cofilin fluorescent immunostaining in PoDG (ipsilateral to virus injection). HA-positive (HA$^+$) and HA-negative (HA$^-$) cells are indicated. **(D)** Representative microphotographs of α-HA fluorescent immunostaining ipsilateral to virus injection (in PoDG) and contralateral to injection (in ML). **(E, F)** The analysis of synaptic responses in ML of the brain slices with eGFP and Cfl (in PoDG or ML). Field excitatory postsynaptic potentials (fEPSPs) were recorded in ML in response to the stimulation of the axons terminating in ML (see Fig. 4C). **(E)** Example of PPR traces of fEPSPs with 25 ms inter-stimulus interval and summary of data for PPR fEPSP slope recorded for different inter-stimulus intervals (25, 50, 100, 200 ms) (repeated measure ANOVA, effect of stimulation intensity, $F_{(2, 123)} = 20.9$, $p < 0.001$; treatment effect, $F_{(3, 123)} = 4.22$, $p = 0.007$; treatment × stimulation interaction, $F_{(6, 123)} = 0.306$, $p = 0.933$). **(E, right)** Summary of data for PPR fEPSP slope recorded for 50 ms interval (one-way ANOVA with Tukey's multiple comparisons test, $F_{(2, 29)} = 9.33$, $p < 0.001$). **(F)** Representative fEPSPs traces evoked by stimuli of different intensities and summary of data for input–output plots of fEPSP slope recorded in response to increasing intensities of stimulation (repeated measure ANOVA, effect of stimulation intensity, $F_{(12, 372)} = 63.8$, $p <0.001$; treatment effect, $F_{(2, 31)} = 2.91$, $p = 0.069$; treatment × stimulation interaction, $F_{(24, 372)} = 2.92$, $p < 0.001$). **(F, top right)** Summary of data for fEPSP slope elicited by 300 μA stimulus (one-way ANOVA with Tukey's multiple comparisons test, $F_{(2, 30)} = 6.16$, $p = 0.006$). **(F, bottom)** Summary of data for fiber volley (FV) amplitude recorded in response to increasing intensities of stimulation (repeated measure three-way ANOVA, AUD: $F_{(1, 38)} = 6.22$, $p = 0.017$; time: $F_{(1, 38)} = 0.162$, $p = 0.689$). **(F, bottom right)** Summary of data for FV amplitude elicited by 300 μA stimulus intensity (repeated measure ANOVA, effect of stimulation intensity, $F_{(1,33, 38,6)} = 149$, $p <0.001$; treatment effect, $F_{(2, 29)} = 0.258$, $p = 0.774$ treatment × stimulation interaction, $F_{(24, 348)} = 0.408$, $p = 0.995$). Data are presented as means +/- SEM. The numbers of analyzed slices are indicated in the legends.

reduced synaptic function in the dentate gyrus (DG) of ≥2 crit drinkers during withdrawal compared to <2 crit animals. Manipulation of Cfl levels in the polymorphic layer of the dentate gyrus (PoDG) influenced aspects of the AUD phenotype, including synaptic function, alcohol motivation, alcohol-seeking behavior during withdrawal, and alcohol consumption during relapse. Similar behavioral effects were observed when sucrose was used as a reward, and the opposite effect when Cfl level was depleted, suggesting a general role for Cfl in the extinction of reward-driven behaviors. Furthermore, analysis of human data identified three SNPs within the CFL1 gene that predicted the AUD phenotype, and blood CFL1 mRNA levels were found to predict the frequency of alcohol-related hospital readmissions.

RNA-seq enables the discovery of novel molecular mechanisms underlying psychiatric disorders. In the context of AUD, extensive transcriptomic analyses have been conducted using either brain tissue from AUD patients [59–61] or animals with a history of alcohol consumption [62–64]. However, these approaches have significant limitations. When analyzing human tissue, it is not possible to distinguish between transcripts contributing to the development of AUD and those altered only during advanced stages of the disease. Conversely, transcriptomic analyses in animal models often compare alcohol-exposed animals with alcohol-naive controls, without diagnosing AUD in the tested subjects. Such comparisons fail to differentiate transcripts specific to alcohol exposure from those involved in AUD progression. Here, we performed the first analysis of transcriptomic differences between AUD-prone and AUD-resistant animals during extinction of alcohol seeking. These groups exhibited significant differences across all tested AUD-related behaviors. We identified over 1000 differentially expressed genes (DEGs) in the hippocampus after alcohol withdrawal. Notably, we observed differences in the transcripts associated with cytoskeletal rearrangement, synaptic function, and the synaptic vesicle cycle.

Several previous studies have linked actin cytoskeleton rearrangement to AUD [65]. These studies primarily associated actin cytoskeleton stabilization with sensitivity to ethanol's sedative effects [66–68] and ethanol consumption [69]. For instance, the local deletion of Prosapip1 (an actin regulatory protein) in the nucleus accumbens reduces F-actin levels in alcohol-treated animals compared to alcohol-treated controls and decreases alcohol consumption [70]. Conversely, mice lacking Eps8 exhibit increased ethanol consumption, and Eps8-null neurons are resistant to the actin-remodeling activity of NMDA receptors and ethanol [67]. Consistent with these findings, we observed that Cfl, a key regulator of F-actin depolymerization and synaptic physiology [70], bidirectionally influences alcohol consumption during relapse and pre-synaptic activity in ML. Overexpression of Cfl reduces the strength of glutamatergic synapses and decreases alcohol consumption, while Cfl knockdown produces the opposite effects.

The role of actin cytoskeleton in the regulation of AUD-related behaviors beyond alcohol consumption remains poorly understood. To our knowledge, only one study so far linked actin-binding protein, Prosapip1, with alcohol seeking and reward [71]. Here we demonstrate that differential expression of the hippocampal transcripts related to actin cytoskeleton distinguishes the ≥ 2 crit and < 2 crit mice during alcohol withdrawal. Specifically, we show that Cfl expression is increased in the DG of the ≥ 2 crit mice during alcohol withdrawal and local manipulation of Cfl in the PoDG bidirectionally affects extinction of alcohol and sucrose seeking during withdrawal. This phenotype is unlikely to be driven by altered reward motivation, as the effect on alcohol motivation is observed only after Cfl overexpression, but not with Cfl knockdown. It is also improbable that the extinction phenotype results from altered reward perception, as Cfl manipulations have opposing effects on reward consumption and extinction of reward seeking. However, it is possible that Cfl influences cognitive processes required to update the value of a reward-associated context. This hypothesis is supported by previous studies showing that DG inactivation impairs the ability to learn changed contingencies in previously encountered environments [72–74]. As we do not see the effect of Cfl on extinction of aversive memories it remains to be established how neuronal mechanisms underlying extinction of aversive and appetitive memories differ.

Paradoxically, manipulation of Cfl in the PoDG affects reward seeking and consumption during relapse in opposite directions. This contradiction likely reflects the complex interplay of multiple neuronal mechanisms underlying different AUD endophenotypes. This notion is supported by our observation that AUD-related behaviors frequently do not correlate with one another, underscoring the need for more personalized approaches in AUD treatment of the patients with different behavioral profiles.

Previously, CFL1 has been implicated in neurodegenerative diseases (e.g., Alzheimer's and Huntington's diseases) [75], neuronal migration disorders (e.g., lissencephaly, epilepsy, and schizophrenia), neural tube closure defects [76], and memory consolidation during sleep [53]. Mutations in CFL1 have been linked to impaired neural crest cell migration and neural tube closure defects [77]. Here, we extend these findings by demonstrating the role of Cfl in regulating core AUD symptoms in an animal model, identifying CFL1 SNPs that contribute to AUD
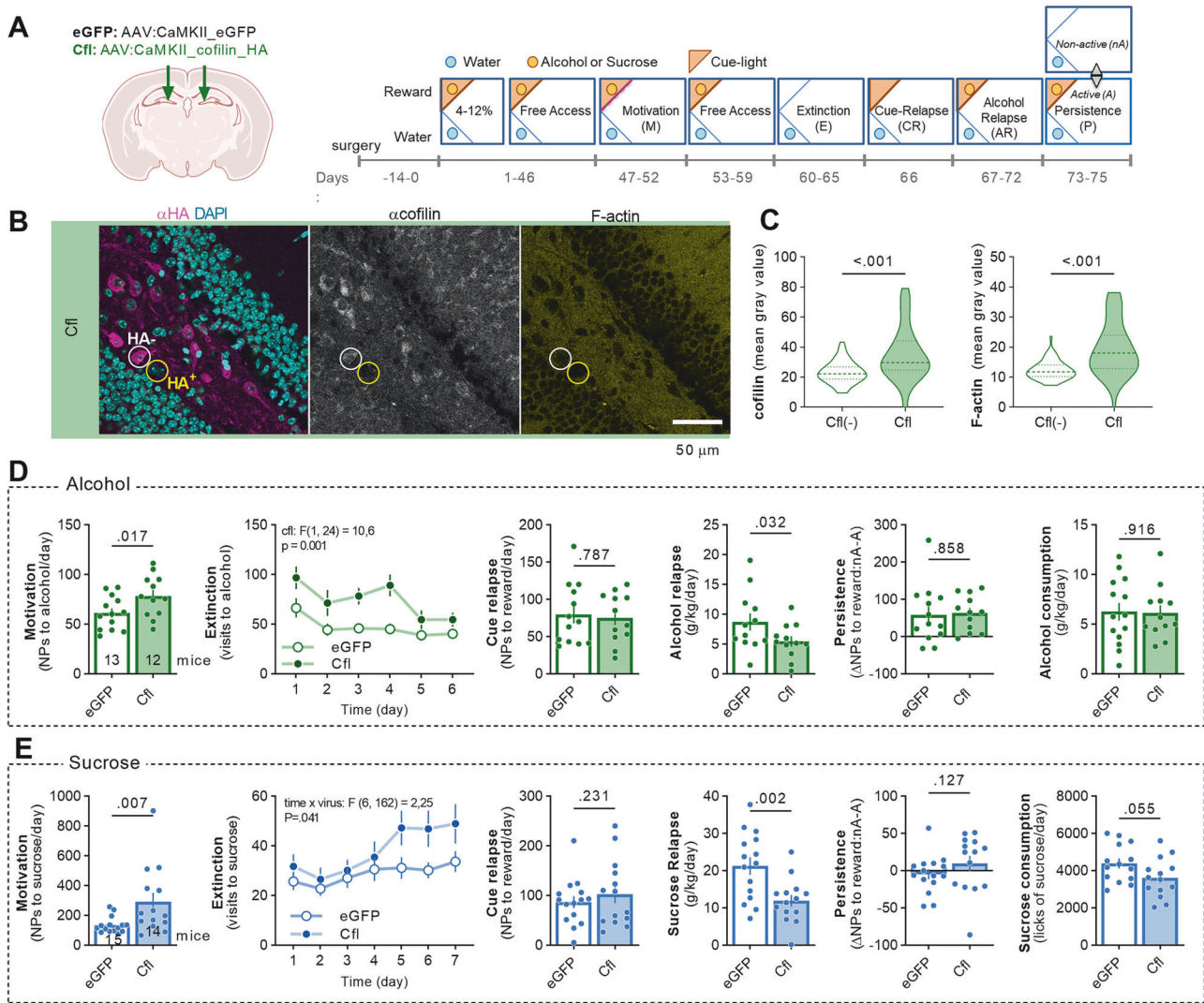
Fig. 6 Overexpression of Cfl in PoDG impairs extinction of reward seeking and increases reward motivation. (A) Experimental timelines and IntelliCage setups. Mice received dDG-targeted bilateral stereotactic injections of AAV2.1 encoding cofilin-HA (n = 26) or eGFP (n = 28). Mice were trained to drink alcohol (4–12% and Free access) or sucrose (5%) and AUD-related behaviors were tested: motivation to drink alcohol (M), alcohol seeking during withdrawal (W) and cue relapse (CR), alcohol drinking during alcohol relapse (AR), and alcohol seeking during a persistence test (P). **(B, C)** The analysis of cofilin and F-actin levels in PoDG cells. **(B)** Representative microphotographs of double immunolabeling with α-HA and α-cofilin, combined with DAPI (nuclear marker) and F-actin fluorescent labeling. **(C)** Summary of data showing cofilin (Mann-Whitney U = 758) and F-actin levels (Mann-Whitney U = 531) in the cells expressing cofilin, or non-transduced PoDG cells analyzed in the same animals [cofilin(-)]. Cells were detected based on DAPI staining. **(D)** Summary of data showing individual scores in AUD-related behaviors: motivation to alcohol (t(24) = 3.09), extinction of alcohol seeking during withdrawal (repeated measures one-way ANOVA, effect of virus: F(1,16) = 5.84, p = 0.028), alcohol seeking during cue relapse (t(24) = 0.455), alcohol consumption during alcohol relapse (t(23) = 1.89), persistence in alcohol seeking (t(24) = 2.12) and alcohol consumption during free access periods (t(24) = 0.107). **(E)** Summary of data showing individual scores in addiction-related behaviors for mice drinking sucrose: motivation to sucrose (t(27) = 2.61), extinction of sucrose seeking during withdrawal (repeated measures ANOVA, time x virus interaction: F(6, 162) = 2.39, p = 0.031), sucrose seeking during cue relapse (t(27) = 0.748), sucrose consumption during relapse (t(27) = 3.24), persistence in sucrose seeking (t(27) = 1.17) and sucrose consumption during free access periods (t(27) = 0.201). Data are presented as means +/- SEM.

risk, and establishing *CFL1* blood mRNA levels as a predictor of hospitalization due to alcohol use. As *CFL1* SNPs producing non-coding transcripts and low *CFL1* mRNA levels are associated with increased AUD risk and hospitalization our human data align with animal studies showing increased alcohol consumption during relapse after Cfl knockdown in the dentate gyrus (DG).

While the effect of actin-binding proteins on alcohol consumption was linked primarily to F-actin stability, the mechanisms by which they affect other AUD behaviors remain largely unknown. In this study, we observed that Cfl overexpression in PoDG increased the paired-pulse ratio (PPR) in contralateral molecular layer (ML) synapses and decreased the fEPSP slope in input-output tests,

indicating impaired ML synapse function likely caused by reduced presynaptic release probability. Similar physiological changes were seen in ≥2 crit mice compared to <2 crit mice following the extinction test. Thus, increased Cfl levels in the ML of ≥2 crit mice likely underlie the synaptic weakening observed during withdrawal. However, we cannot rule out that *Cfl* in PoDG also affects other projections.

In its unphosphorylated, active state, cofilin severs actin filaments, increasing actin cytoskeletal dynamics [48]. This mechanism regulates both postsynaptic function and synaptic vesicle mobilization/exocytosis [49–51]. Active Cfl may also bind to F-actin, forming stable actin rods that block axonal trafficking [52].
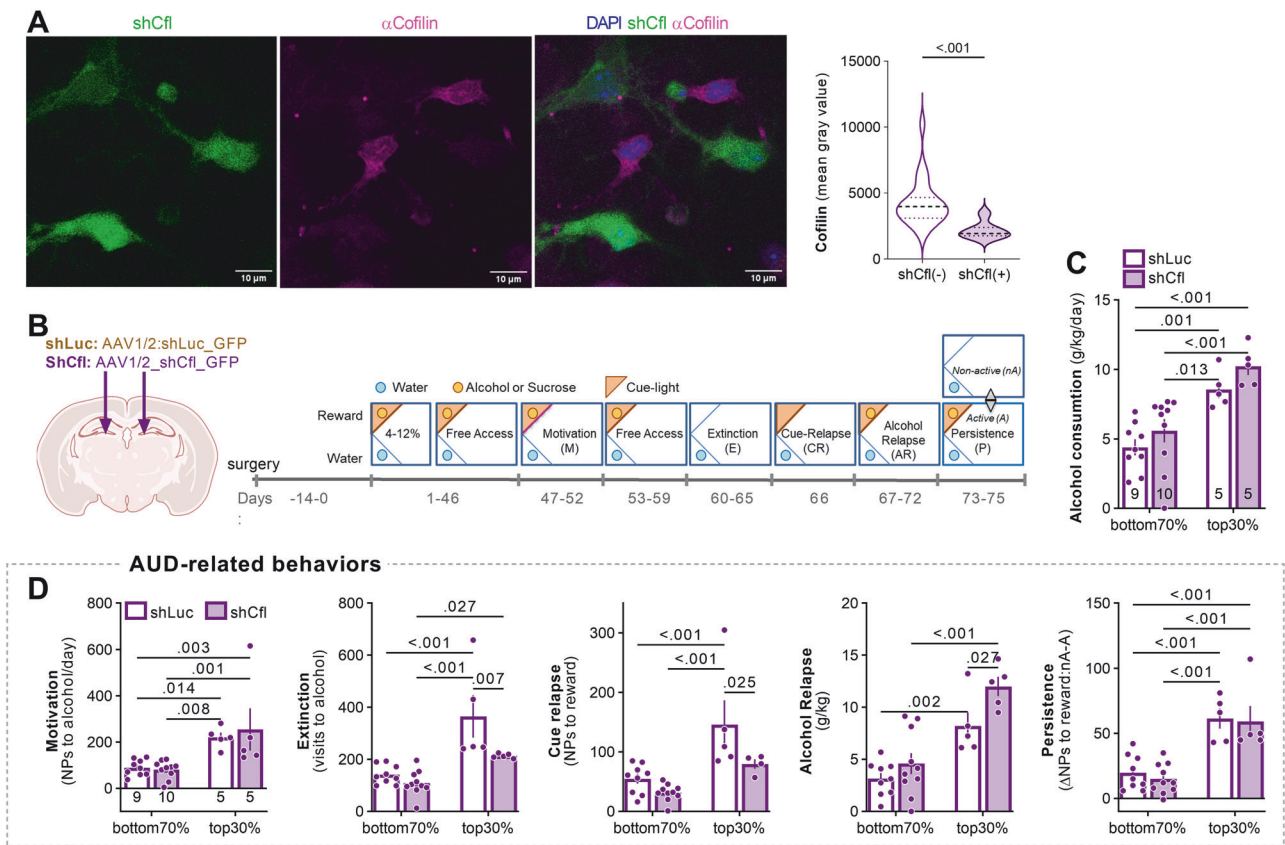
Fig. 7 Downregulation of Cfl in DG decreases alcohol seeking during extinction and cue relapse, and increases alcohol consumption during relapse. (A) The analysis of shCfl efficiency. Representative microphotographs of double immunolabeling with α-GFP and α-cofilin, combined with DAPI (nuclear marker) in the primary hippocampal cells culture, and summary of data showing cofilin levels in the neurons expressing shCfl (n = 21), or non-transduced neurons (n = 18) (Mann-Whitney U = 32). Cells were detected based on DAPI staining. **(B)** Experimental timelines and IntelliCage setups. Mice received dDG-targeted bilateral stereotactic injections of LVs encoding shCfl (n = 15) or shLuc (n = 14). Mice were trained to drink alcohol (4–12% and Free access) and AUD-related behaviors were tested: motivation to drink alcohol (M), alcohol seeking during withdrawal (W) and cue relapse (CR), alcohol drinking during alcohol relapse (AR), and alcohol seeking during a persistence test (P). **(C, D)** Summary of data showing individual scores in alcohol consumption during free access periods **(C)** and AUD-related behaviors **(D)**. The animals were divided into two groups (bottom 70% and top 30% of the population) based on their performance in the tests. A significant effect of shCfl was observed on extinction of alcohol seeking during withdrawal (two-way ANOVA and LSD *post hoc* tests, effect of virus: $F(1, 25) = 8.37$, $p = 0.008$), alcohol seeking during cue relapse ($F(1, 24) = 7.08$, $p = 0.014$), and alcohol consumption during alcohol relapse ($F(1, 25) = 6.87$, $p = 0.015$). We found no effect of shCfl on motivation to alcohol ($F(1, 25) = 0.141$, $p = 0.711$), persistence in alcohol seeking ($F(1, 25) = 0.299$, $p = 0.589$) and alcohol consumption during free access periods ($F(1, 25) = 3.30$, $p = 0.081$). Data are presented as means +/- SEM.

These processes may explain the impaired ML synapse function observed in alcohol-naive mice with Cfl overexpression and in ≥2 crit mice during withdrawal. The role of pre-synaptic compartments in the hippocampus in the regulation of extinction of alcohol seeking is also supported by our RNA-seq data showing differential expression of the genes related to axonal projections and synaptic vesicle cycle between the ≥ 2 crit and < 2 crit mice. Alternatively, Cfl may impair the DG circuit by inhibiting PoDG postsynaptic compartments, though this is less likely, as we found no significant changes in Cfl colocalization with PSD-95 in ≥2 crit mice after extinction.

Our findings build on previous studies linking impaired DG synaptic transmission and morphology to AUD-related behaviors [32, 33]. Previously, we found that the addicted phenotype is characterised by the generation of thin (likely immature) dendritic spines in DG during alcohol withdrawal [32] and the frequency of silent synapses (lacking functional AMPA receptors) generated during cue relapse in the ML correlates positively with the AUD index [32]. Here, we expand these findings by demonstrating Cfl's role in PoDG in regulating alcohol and sucrose motivation and the extinction of alcohol and sucrose seeking during withdrawal. These results also align with earlier studies highlighting the DG's

role in drug and reward motivation [38, 39, 78]. Moreover, previous research has implicated DG granule cells in fear memory extinction and learning contextual contingencies [54, 74, 79]. However, our data suggest that Cfl in PoDG does not affect contextual fear memory formation or extinction, possibly reflecting functional differences between dorsal DG granule cells and PoDG mossy cells.

Overall, by combining a multidimensional AUD animal model with genomic, electrophysiological, and biochemical analyses, we identified a novel molecular mechanism underlying increased alcohol motivation and impaired extinction of alcohol-seeking during withdrawal. This mechanism, specific to individuals prone to AUD behaviors, involves upregulation of Cfl at DG presynapses, resulting in weakened synaptic transmission during alcohol withdrawal. Additionally, we demonstrated the role of Cfl in alcohol consumption during relapse and identified three SNPs within the human CFL1 gene that increase AUD risk. Blood CFL1 mRNA levels were also found to predict the frequency of alcohol-related hospital admissions in AUD patients. Collectively, these findings may inform the development of novel therapeutic strategies targeting synaptic transmission in AUD patients.

Table 1. Correlations between blood Cfl mRNA levels and demographic data in human AUD patients (NOAH study).

	r	p
Control		
Age	0.085	0.224
BMI	0.021	0.768
AUDIT score	0.024	0.744
AUD patients at admission		
Age	−0.150	0.036
BMI	0.073	0.333
PACS score	0.084	0.257
Lifetime drinking (kg)	−0.028	0.733
Daily ethanol intake (kg)	−0.102	0.227
Number of alcohol-related readmissions during follow-up	0.013	0.859
Days to first alcohol-related readmission during follow-up	−0.075	0.297
OCDS score	0.113	0.126
AUD patients after 5-day detoxification		
Age	−0.109	0.176
BMI	−0.026	0.752
PACS score	0.083	0.309
Lifetime drinking (kg)	0.023	0.803
Daily ethanol intake (kg)	0.064	0.489
Number of alcohol-related readmissions during follow-up	−0.244	0.002
Days to first alcohol-related readmission during follow-up	0.205	0.010
OCDS score	0.138	0.093

DATA AVAILABILITY

RNAseq data is available at GEO NCBI (GSE221166). The other datasets generated during the current study are available at Open Science Framework (https://osf.io/crmus).

REFERENCES

1. Diagnostic and statistical manual of mental disorders: DSM-5. 5th ed. Washington, D.C: American Psychiatric Association; 2013.
2. Carvalho AF, Heilig M, Perez A, Probst C, Rehm J. Alcohol use disorders. The Lancet. 2019;394:781–92.
3. Glantz MD, Bharat C, Degenhardt L, Sampson NA, Scott KM, Lim CCW, et al. The epidemiology of alcohol use disorders cross-nationally: findings from the World Mental Health Surveys. Addict Behav. 2020;102:106128.
4. Jonas DE, Amick HR, Feltner C, Bobashev G, Thomas K, Wines R, et al. Pharmacotherapy for adults with alcohol use disorders in outpatient settings: a systematic review and meta-analysis. JAMA. 2014;311:1889–1900.
5. Ron D, Barak S. Molecular mechanisms underlying alcohol-drinking behaviours. Nat Rev Neurosci. 2016;17:576–91.
6. Kranzler HR, Zhou H, Kember RL, Vickers Smith R, Justice AC, Damrauer S, et al. Genome-wide association study of alcohol consumption and use disorder in 274,424 individuals from multiple populations. Nat Commun. 2019;10:1499.
7. Egervari G, Siciliano CA, Whiteley EL, Ron D. Alcohol and the brain: from genes to circuits. Trends Neurosci. 2021;44:1004–15.
8. Gelernter J, Polimanti R. Genetics of substance use disorders in the era of big data. Nat Rev Genet. 2021;22:712–29.
9. GESGA Consortium, Levey DF, Le-Niculescu H, Frank J, Ayalew M, Jain N, et al. Genetic risk prediction and neurobiological understanding of alcoholism. Transl Psychiatry. 2014;4:e391–e391.
10. Siciliano CA, Noamany H, Chang C-J, Brown AR, Chen X, Leible D, et al. A cortical-brainstem circuit predicts and governs compulsive alcohol drinking. Science. 2019;366:1008–12.
11. Domi E, Xu L, Toivainen S, Nordeman A, Gobbo F, Venniro M, et al. A neural substrate of compulsive alcohol use. Sci Adv. 2021;7:eabg9045.
12. Seif T, Chang S-J, Simms JA, Gibb SL, Dadgar J, Chen BT, et al. Cortical activation of accumbens hyperpolarization-active NMDARs mediates aversion-resistant alcohol intake. Nat Neurosci. 2013;16:1094–1100.
13. Giuliano C, Belin D, Everitt BJ. Compulsive alcohol seeking results from a failure to disengage dorsolateral striatal control over behavior. J Neurosci. 2019;39:1744–54.
14. Goutaudier R, Joly F, Mallet D, Bartolomucci M, Guicherd D, Carcenac C, et al. Hypodopaminergic state of the nigrostriatal pathway drives compulsive alcohol use. Mol Psychiatry. 2023;28:463–74.
15. Pfarr S, Meinhardt MW, Klee ML, Hansson AC, Vengeliene V, Schönig K, et al. Losing control: excessive alcohol seeking after selective inactivation of cue-responsive neurons in the infralimbic cortex. J Neurosci Off J Soc Neurosci. 2015;35:10750–61.
16. Augier E, Barbier E, Dulman RS, Licheri V, Augier G, Domi E, et al. A molecular mechanism for choosing alcohol over an alternative reward. Science. 2018;360:1321–6.
17. Augier G, Schwabl V, Lguensat A, Atudorei M, Iyere OC, Solander SE, et al. Wistar rats choose alcohol over social interaction in a discrete-choice model. Neuropsychopharmacol Off Publ Am Coll Neuropsychopharmacol. 2023;48:1098–107.
18. Marchant NJ, McDonald AJ, Matsuzaki R, van Mourik Y, Schetters D, De Vries TJ. Rats choose alcohol over social reward in an operant choice procedure. Neuropsychopharmacol Off Publ Am Coll Neuropsychopharmacol. 2023;48:585–93.
19. Wilcox CE, Dekonenko CJ, Mayer AR, Bogenschutz MP, Turner JA. Cognitive control in alcohol use disorder: deficits and clinical relevance. Rev Neurosci. 2014;25:1–24.
20. Chesworth R, Corbit LH. Recent developments in the behavioural and pharmacological enhancement of extinction of drug seeking. Addict Biol. 2017;22:3–43.
21. LeCocq MR, Randall PA, Besheer J, Chaudhri N. Considering drug-associated contexts in substance use disorders and treatment development. Neurother J Am Soc Exp Neurother. 2020;17:43–54.
22. Marchant NJ, Campbell EJ, Pelloux Y, Bossert JM, Shaham Y. Context-induced relapse after extinction versus punishment: similarities and differences. Psychopharmacology (Berl). 2019;236:439–48.
23. Millan EZ, Marchant NJ, McNally GP. Extinction of drug seeking. Behav Brain Res. 2011;217:454–62.
24. Domi E, Domi A, Adermark L, Heilig M, Augier E. Neurobiology of alcohol seeking behavior. J Neurochem. 2021;157:1585–614.
25. Chaudhri N, Sahuque LL, Cone JJ, Janak PH. Reinstated ethanol-seeking in rats is modulated by environmental context and requires the nucleus accumbens core. Eur J Neurosci. 2008;28:2288–98.
26. Hamlin AS, Newby J, McNally GP. The neural correlates and role of D1 dopamine receptors in renewal of extinguished alcohol-seeking. Neuroscience. 2007;146:525–36.
27. Fuchs RA, Evans KA, Ledford CC, Parker MP, Case JM, Mehta RH, et al. The role of the dorsomedial prefrontal cortex, basolateral amygdala, and dorsal hippocampus in contextual reinstatement of cocaine seeking in rats. Neuropsychopharmacol Off Publ Am Coll Neuropsychopharmacol. 2005;30:296–309.
28. Fuchs RA, Eaddy JL, Su Z-I, Bell GH. Interactions of the basolateral amygdala with the dorsal hippocampus and dorsomedial prefrontal cortex regulate drug context-induced reinstatement of cocaine-seeking in rats: Limbic interactions in contextual cocaine-seeking. Eur J Neurosci. 2007;26:487–98.
29. Ramirez DR, Bell GH, Lasseter HC, Xie X, Traina SA, Fuchs RA. Dorsal hippocampal regulation of memory reconsolidation processes that facilitate drug context-induced cocaine-seeking behavior in rats. Eur J Neurosci. 2009;30:901–12.
30. Campbell EJ, Lawrence AJ. It's more than just interoception: The insular cortex involvement in alcohol use disorder. J Neurochem. 2021;157:1644–51.
31. Radwanska K, Kaczmarek L. Characterization of an alcohol addiction-prone phenotype in mice: characterization of an alcohol addiction-prone phenotype. Addict Biol. 2012;17:601–12.
32. Beroun A, Nalberczak-Skóra M, Harda Z, Piechota M, Ziółkowska M, Cały A, et al. Generation of silent synapses in dentate gyrus correlates with development of alcohol addiction. Neuropsychopharmacology. 2018;43:1989–99.
33. Nalberczak-Skóra M, Beroun A, Skonieczna E, Cały A, Ziółkowska M, Pagano R, et al. Impaired synaptic transmission in dorsal dentate gyrus increases impulsive alcohol seeking. Neuropsychopharmacol Off Publ Am Coll Neuropsychopharmacol. 2022. 1 October 2022. https://doi.org/10.1038/s41386-022-01464-5.
34. Pagano R, Salamian A, Zielinski J, Beroun A, Nalberczak-Skóra M, Skonieczna E, et al. Arc controls alcohol cue relapse by a central amygdala mechanism. Mol Psychiatry. 2023;28:733–45.
35. Stefaniuk M, Beroun A, Lebitko T, Markina O, Leski S, Meyza K, et al. Matrix Metalloproteinase-9 and synaptic plasticity in the central amygdala in control of alcohol-seeking behavior. Biol Psychiatry. 2017;81:907–17.
36. Mijakowska Z, Łukasiewicz K, Ziółkowska M, Lipiński M, Trąbczyńska A, Matuszek Ż, et al. Autophosphorylation of alpha isoform of calcium/calmodulin-dependent

kinase II regulates alcohol addiction-related behaviors. Addict Biol. 2017;22:331–41.

37. Marchant NJ, Campbell EJ, Whitaker LR, Harvey BK, Kaganovsky K, Adhikary S, et al. Role of ventral subiculum in context-induced relapse to alcohol seeking after punishment-imposed abstinence. J Neurosci. 2016;36:3281–94.

38. Noonan MA, Bulin SE, Fuller DC, Eisch AJ. Reduction of adult hippocampal neurogenesis confers vulnerability in an animal model of cocaine addiction. J Neurosci. 2010;30:304–15.

39. Deroche-Gamonet V, Revest J-M, Fiancette J-F, Balado E, Koehl M, Grosjean N, et al. Depleting adult dentate gyrus neurogenesis increases cocaine-seeking behavior. Mol Psychiatry. 2019;24:312–20.

40. Trouche S, Koren V, Doig NM, Ellender TJ, El-Gaby M, Lopes-dos-Santos V, et al. A Hippocampus-Accumbens tripartite neuronal motif guides appetitive memory in space. Cell. 2019;176:1393–1406.e16.

41. Meyers RA, Zavala AR, Neisewander JL. Dorsal, but not ventral, hippocampal lesions disrupt cocaine place conditioning. NeuroReport. 2003;14:2127–31.

42. Meyers RA, Zavala AR, Speer CM, Neisewander JL. Dorsal hippocampus inhibition disrupts acquisition and expression, but not consolidation, of cocaine conditioned place preference. Behav Neurosci. 2006;120:401–12.

43. Bamburg JR. Proteins of the ADF/Cofilin family: essential regulators of actin dynamics. Annu Rev Cell Dev Biol. 1999;15:185–230.

44. Shaham Y, Shalev U, Lu L, de Wit H, Stewart J. The reinstatement model of drug relapse: history, methodology and major findings. Psychopharmacology (Berl). 2003;168:3–20.

45. Deroche-Gamonet V. Evidence for addiction-like behavior in the rat. Science. 2004;305:1014–7.

46. Ge SX, Jung D, Yao R. ShinyGO: a graphical gene-set enrichment tool for animals and plants. Bioinforma Oxf Engl. 2020;36:2628–9.

47. Kanehisa M, Goto S, Furumichi M, Tanabe M, Hirakawa M. KEGG for representation and analysis of molecular networks involving diseases and drugs. Nucleic Acids Res. 2010;38:D355–360.

48. Maciver SK, Hussey PJ. The ADF/cofilin family: actin-remodeling proteins. Genome Biol. 2002;3:reviews3007.1.

49. Morales M, Colicos MA, Goda Y. Actin-dependent regulation of neurotransmitter release at central synapses. Neuron. 2000;27:539–50.

50. Zimmermann A-M, Jene T, Wolf M, Görlich A, Gurniak CB, Sassoè-Pognetto M, et al. Attention-Deficit/Hyperactivity disorder–like phenotype in a mouse model with impaired actin dynamics. Biol Psychiatry. 2015;78:95–106.

51. Wolf M, Zimmermann A-M, Görlich A, Gurniak CB, Sassoè-Pognetto M, Friauf E, et al. ADF/Cofilin controls synaptic actin dynamics and regulates synaptic vesicle mobilization and exocytosis. Cereb Cortex. 2015;25:2863–75.

52. Minamide LS, Striegl AM, Boyle JA, Meberg PJ, Bamburg JR. Neurodegenerative stimuli induce persistent ADF/cofilin–actin rods that disrupt distal neurite function. Nat Cell Biol. 2000;2:628–36.

53. Havekes R, Park AJ, Tudor JC, Luczak VG, Hansen RT, Ferri SL, et al. Sleep deprivation causes memory deficits by negatively impacting neuronal connectivity in hippocampus area CA1. eLife. 2016;5:e13424.

54. Khalaf O, Resch S, Dixsaut L, Gorden V, Glauser L, Gräff J. Reactivation of recall-induced neurons contributes to remote fear memory attenuation. Science. 2018;360:1239–42.

55. Vengeliene V, Kiefer F, Spanagel R. d-Cycloserine facilitates extinction of conditioned alcohol-seeking behaviour in rats. Alcohol Alcohol. 2008;43:626–9.

56. Leung HT, Corbit LH. Extinction of alcohol seeking is enhanced by compound extinction and the noradrenaline reuptake inhibitor atomoxetine. Addict Biol. 2017;22:47–57.

57. Kaminski BJ, Duke AN, Weerts EM. Effects of naltrexone on alcohol drinking patterns and extinction of alcohol seeking in baboons. Psychopharmacology (Berl). 2012;223:55–66.

58. Bouton ME, Maren S, McNally GP. Behavioral and neurobiological mechanisms of pavlovian and instrumental extinction learning. Physiol Rev. 2021;101:611–81.

59. Brenner E, Tiwari GR, Kapoor M, Liu Y, Brock A, Mayfield RD. Single cell transcriptome profiling of the human alcohol-dependent brain. Hum Mol Genet. 2020;29:1144–53.

60. Enoch M-A, Rosser AA, Zhou Z, Mash DC, Yuan Q, Goldman D. Expression of glutamatergic genes in healthy humans across 16 brain regions; altered expression in the hippocampus after chronic exposure to alcohol or cocaine. Genes Brain Behav. 2014;13:758–68.

61. Maiya R, Pomrenze MB, Tran T, Tiwari GR, Beckham A, Paul MT, et al. Differential regulation of alcohol consumption and reward by the transcriptional cofactor LMO4. Mol Psychiatry. 2021;26:2175–86.

62. Warden AS, Wolfe SA, Khom S, Varodayan FP, Patel RR, Steinman MQ, et al. Microglia control escalation of drinking in alcohol-dependent mice: genomic and synaptic drivers. Biol Psychiatry. 2020;88:910–21.

63. Barbier E, Tapocik JD, Juergens N, Pitcairn C, Borich A, Schank JR, et al. DNA methylation in the medial prefrontal cortex regulates alcohol-induced behavior and plasticity. J Neurosci Off J Soc Neurosci. 2015;35:6153–64.

64. Bogenpohl JW, Smith ML, Farris SP, Dumur CI, Lopez MF, Becker HC, et al. Cross-Species co-analysis of prefrontal cortex chronic ethanol transcriptome responses in mice and monkeys. Front Mol Neurosci. 2019;12:197.

65. Gorini G, Adron Harris R, Dayne Mayfield R. Proteomic approaches and identification of novel therapeutic targets for alcoholism. Neuropsychopharmacology. 2014;39:104–30.

66. Rothenfluh A, Threlkeld RJ, Bainton RJ, Tsai LT-Y, Lasek AW, Heberlein U. Distinct behavioral responses to ethanol are regulated by alternate RhoGAP18B Isoforms. Cell. 2006;127:199–211.

67. Offenhäuser N, Castelletti D, Mapelli L, Soppo BE, Regondi MC, Rossi P, et al. Increased ethanol resistance and consumption in Eps8 knockout mice correlates with altered actin dynamics. Cell. 2006;127:213–26.

68. Peru Y Colón de Portugal RL, Acevedo SF, Rodan AR, Chang LY, Eaton BA, Rothenfluh A. Adult neuronal Arf6 controls ethanol-induced behavior with Arfaptin downstream of Rac1 and RhoGAP18B. J Neurosci Off J Soc Neurosci. 2012;32:17706–13.

69. Ojelade SA, Jia T, Rodan AR, Chenyang T, Kadrmas JL, Cattrell A, et al. Rsu1 regulates ethanol consumption in Drosophila and humans. Proc Natl Acad Sci. 2015;112:E4085–E4093.

70. Ben Zablah Y, Merovitch N, Jia Z. The role of ADF/Cofilin in synaptic physiology and Alzheimer's disease. Front Cell Dev Biol. 2020;8:594998.

71. Laguesse S, Morisot N, Shin JH, Liu F, Adrover MF, Sakhai SA, et al. Prosapip1-Dependent synaptic adaptations in the nucleus accumbens drive alcohol intake, seeking, and reward. Neuron. 2017;96:145–159.e8.

72. Kheirbek MA, Drew LJ, Burghardt NS, Costantini DO, Tannenholz L, Ahmari SE, et al. Differential control of learning and anxiety along the dorsoventral axis of the dentate gyrus. Neuron. 2013;77:955–68.

73. Madroñal N, Delgado-García JM, Fernández-Guizán A, Chatterjee J, Köhn M, Mattucci C, et al. Rapid erasure of hippocampal memory following inhibition of dentate gyrus granule cells. Nat Commun. 2016;7:10923.

74. Bernier BE, Lacagnina AF, Ayoub A, Shue F, Zemelman BV, Krasne FB, et al. Dentate gyrus contributes to retrieval as well as encoding: evidence from context fear conditioning, recall, and extinction. J Neurosci. 2017;37:6359–71.

75. Bamburg JR, Bernstein BW, Davis RC, Flynn KC, Goldsbury C, Jensen JR, et al. ADF/Cofilin-actin rods in neurodegenerative diseases. Curr Alzheimer Res. 2010;7:241–50.

76. Namme JN, Bepari AK, Takebayashi H. Cofilin signaling in the CNS physiology and neurodegeneration. Int J Mol Sci. 2021;22:10727.

77. Bellenchi GC, Gurniak CB, Perlas E, Middei S, Ammassari-Teule M, Witke W. N-cofilin is associated with neuronal migration disorders and cell cycle control in the cerebral cortex. Genes Dev. 2007;21:2347–57.

78. Wolosin SM, Zeithamova D, Preston AR. Reward modulation of hippocampal subfield activation during successful associative encoding and retrieval. J Cogn Neurosci. 2012;24:1532–47.

79. Lacagnina AF, Brockway ET, Crovetti CR, Shue F, McCarty MJ, Sattler KP, et al. Distinct hippocampal engrams control extinction and relapse of fear memory. Nat Neurosci. 2019;22:753–61.

ACKNOWLEDGEMENTS

AUTHOR CONTRIBUTIONS

FUNDING

COMPETING INTERESTS

The authors declare no competing interests.

ADDITIONAL INFORMATION

Publisher's note Springer Nature remains neutral with regard to jurisdictional claims in published maps and institutional affiliations.